Electronic Supplementary Material (ESI) for RSC Advances.

Diols-responsive triple-component supra-amphiphile constructed from pillar[5]arene-based recognition

Bin Hua, Li Shao, Jiong Zhou and Guocan Yu*

State Key Laboratory of Chemical Engineering, Department of Chemistry, Zhejiang University, Hangzhou 310027, P. R. China; Fax and Tel: +86-571-8795-3189;

Email address: guocanyu@zju.edu.cn

Electronic Supplementary Information (16 pages)

1. Materials and methods

All reagents were commercially available and used as received. Compound **1** [S1] and water-soluble pillar[5]arenes[S2] (**WSP5)** were synthesized according to published literature procedures. Solvents were employed as purchased or dried according to procedures described in the published literature.

NMR spectra were obtained on a Bruker Avance III-400 spectrometry or a Bruker AVANCE DMX-500 spectrometer with the internal standard TMS. Isothermal titration calorimetric (ITC) experiments were performed on a VP-ITC micro-calorimeter (Microcal, USA). Low-resolution electrosprayionization mass spectra were recorded with a Bruker Esquire 3000 Plus spectrometer. High-resolution mass spectrometry experiments were performed with a BrukerDaltonics Apex III spectrometer. The melting points were collected on a SHPSIC WRS-2 automatic melting point apparatus. The critical aggregation concentration (CAC) values of **A, G1@A** and **WSP5⊃G1@A** were determined on a DDS-307 instrument. Transmission electron microscopy (TEM) investigation was carried out on a JEM-1200EX instrument. The fluorescence experiments were conducted on a RF-5301 spectrofluorophotometer (ShimadzuCorporation, Japan). Dynamic light scattering measurements were performed on a goniometer ALV/CGS-3 instrument.

For TEM sample preparation, a few drops of the solution were placed on the carbon coated copper grid. Then the solvent was removed by vacuum drying under low temperature to afford the TEM samples.For AFM and SEM sample preparation, a few drops of the solution were placed on the silicon wafer. Then the solvent was removed by vacuum drying under low temperature to afford the TEM samples.

*2. Synthesis of compound **2***

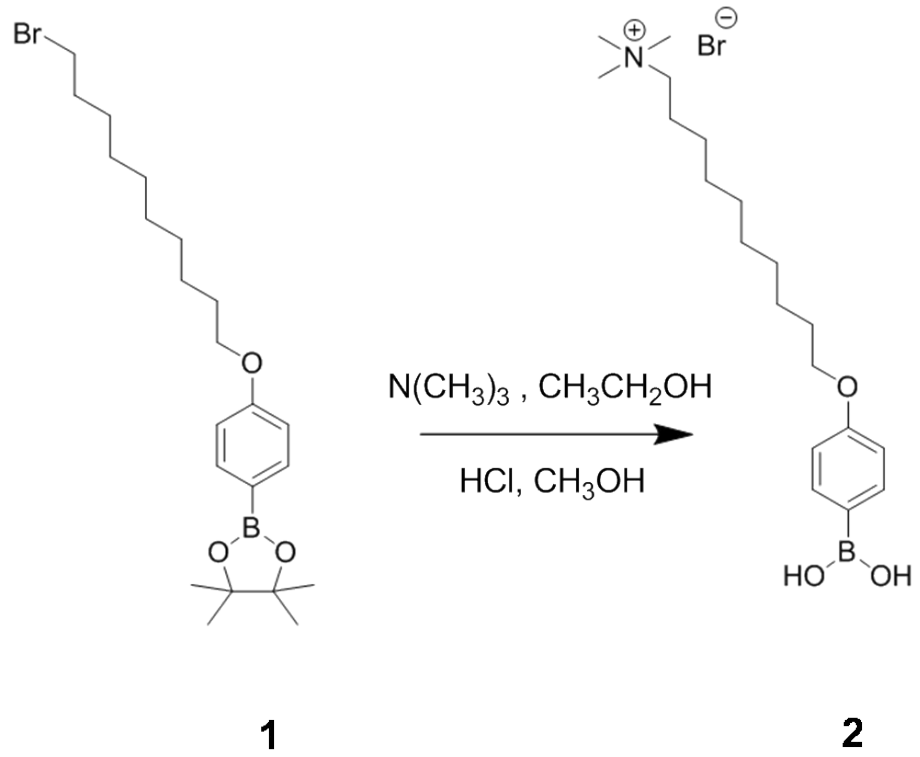

Scheme S1. Synthesis of compound **2**.

Trimethylamine (33 % in ethanol, 5 mL) and compound **1** (438 mg, 1.00 mmol) were added into ethanol (50 mL), and the solution was refluxed for 12 h. The solvents and excess trimethylamine were evaporated under vacuum, and the residues were dissolved in methanol. Then the solution was acidified with aqueous HCl solution. The resulting precipitate was filtered, washed with water, and dried to afford product **2** as a white solid, mp: 233.7−234.5 ºC. The ^{1}H NMR spectrum of **2** is shown in Fig. S1. ^{1}H NMR (400 MHz, CD_3OD, 298 K) δ (ppm): 7.61 (d, J = 8 Hz, 2H), 6.83 (d, J = 8 Hz, 2H), 3.93 (d, J = 8 Hz, 2H), 3.30−3.26 (m, 4H), 3.08 (s, 9H), 1.77−1.69 (m, 4H), 1.46−1.33 (m, 12H). The ^{13}C NMR spectrum of **2** is shown in Fig. S2. ^{13}C NMR (100 MHz, CD_3OD, 298 K) δ (ppm): 162.32, 136.63, 114.68, 68.70, 67.86, 53.54, 30.53, 30.43, 30.40, 30.38, 30.18, 27.35, 27.14, 25.21, 23.95. LRESIMS is shown in shown in Fig. S3: *m/z* 336.5 $[M - Br]^+$. *m/z* calcd for $[M - Br]^+$ $C_{19}H_{35}BNO_3^+$, 336.2705, found 336.2719, error 4 ppm.

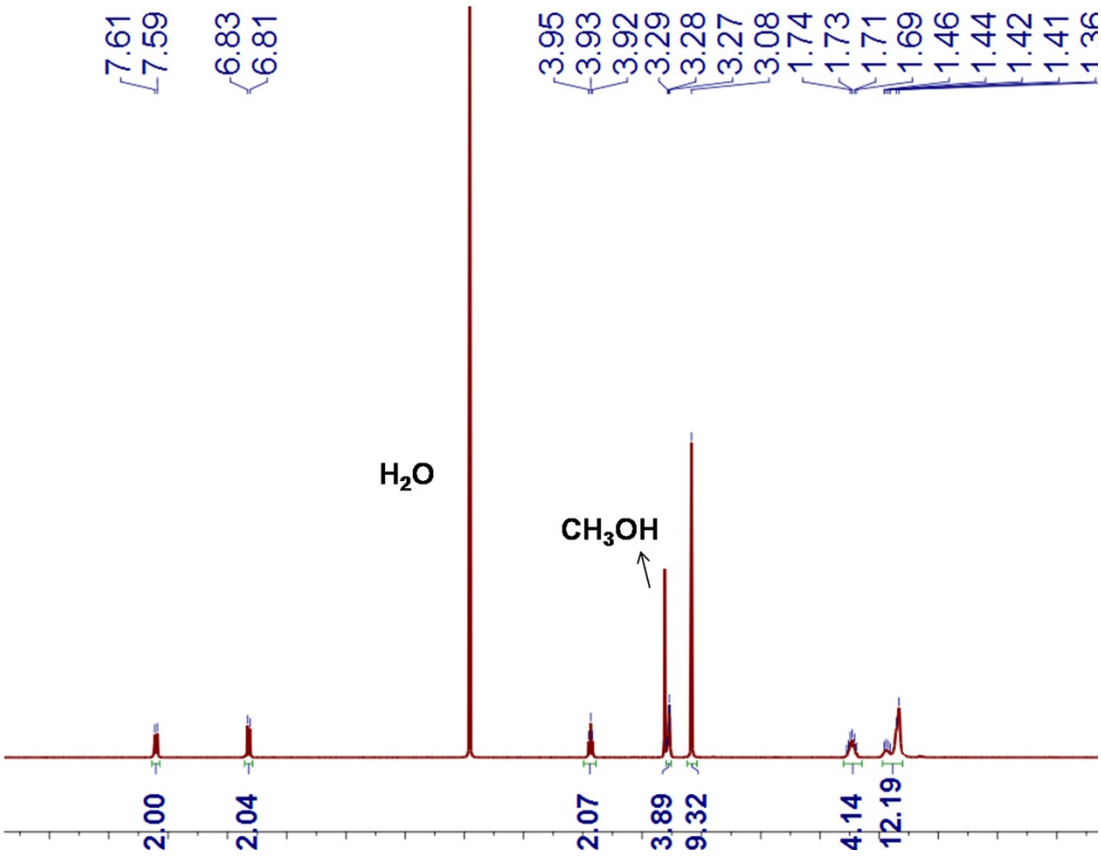

Fig. S1. ^{1}H NMR spectrum (400MHz, CD_3OD, 293K) of **2**.

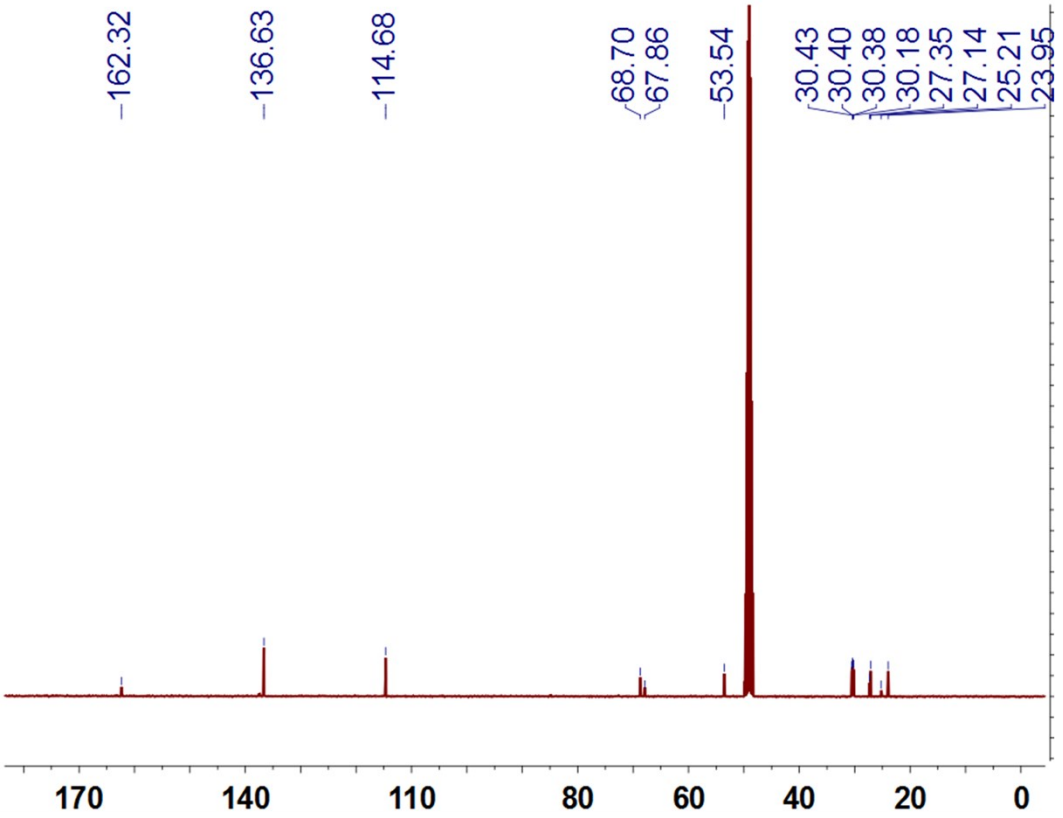

Fig. S2. ^{13}C NMR spectrum (100MHz, CD_3OD, 293K) of **2**.

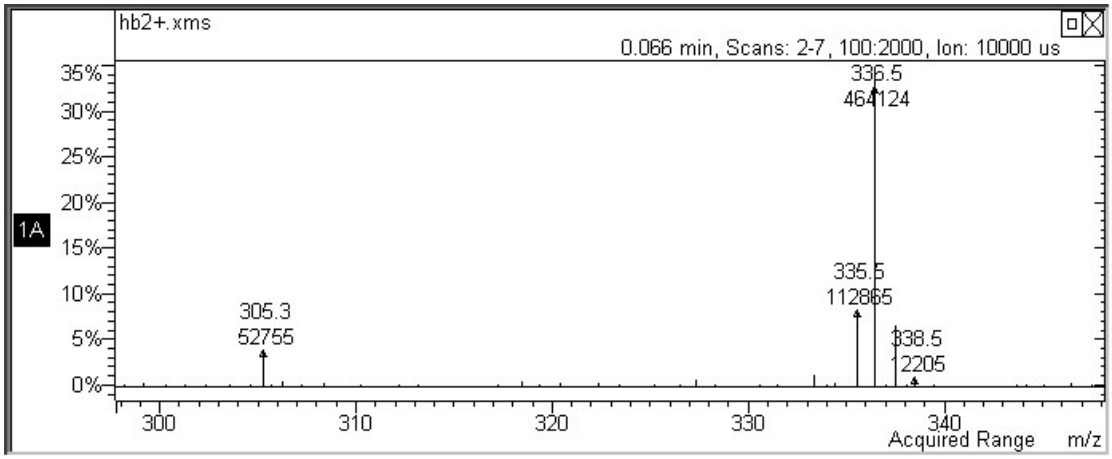

Fig. S3. Electrospray ionization mass spectrum of compound **2**. Assignment of the main peak: *m*/*z* 336.5 $[M - Br]^+$.

*3. Host–guest complexion between **WSP5** and **G2** in D_2O*

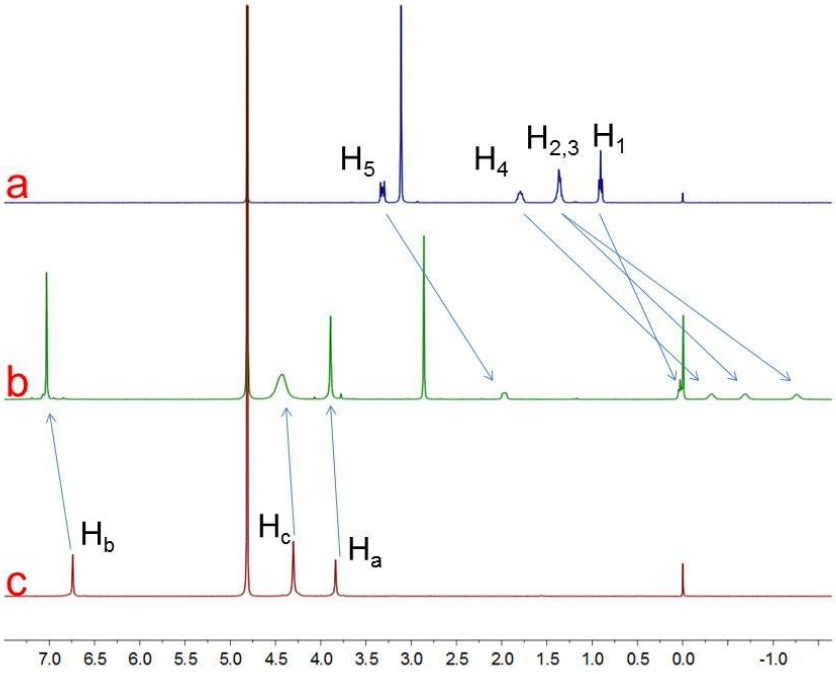

Fig. S4. ^{1}H NMR spectrum (400 MHz, D_2O, room temperature) of solution of **G2** and **WSP5:** (a) **G2** (2.00 mM), (b) the 1:1 mixture of **G2** and **WSP5** (2.00 mM) and (c) **WSP5** (2.00 mM)**.**

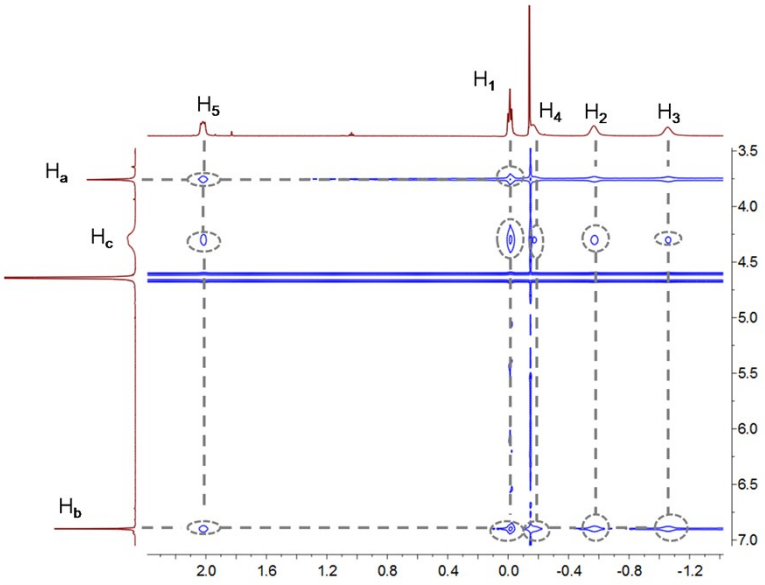

Fig. S5. Partial NOESY NMR spectrum (500 MHz, D_2O, 298 K) of **WSP5 (**10.0 mM) and **G2 (**10.0 mM).

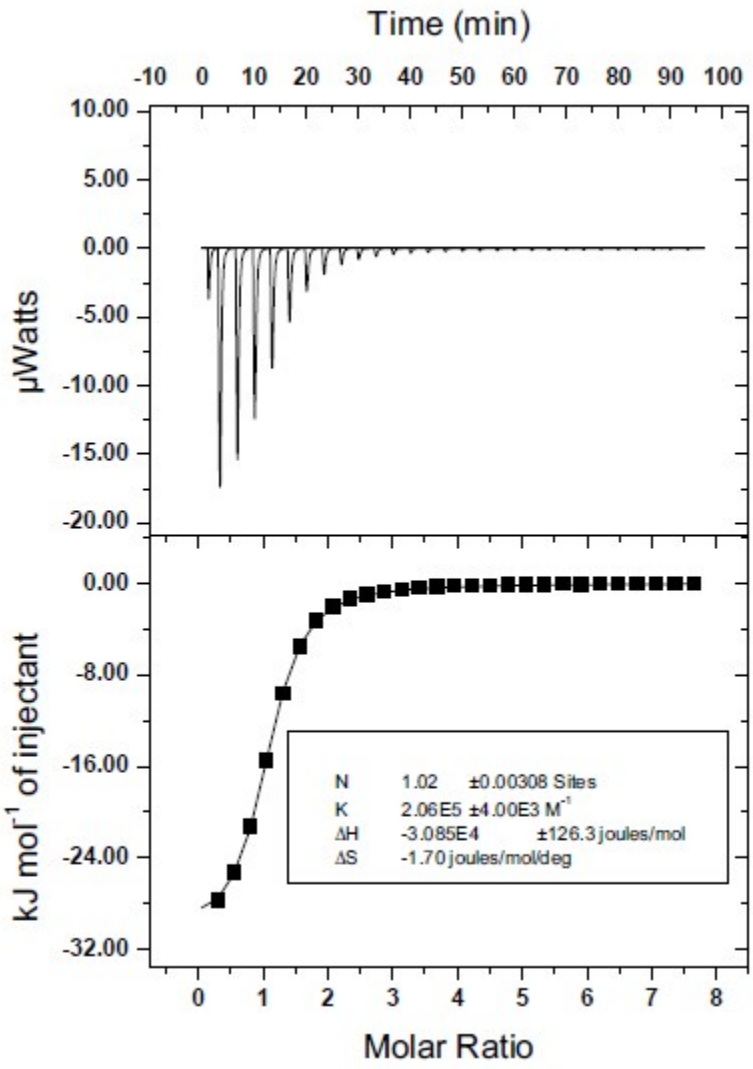

Fig. S6. Microcalorimetric titration of **G2** with **WSP5** in water at 298.15 K. (Top) Raw ITC data for 29 sequential injections (10 µL per injection) of a **G2** solution (2.00 mM) into a **WSP5** solution (0.100 mM). (Bottom) Net reaction heat obtained from the integration of the calorimetric traces.

4 Critical aggregation comcentration (CAC) determination of ***A, G1@A*** *and*

WSP5⊃G1@A

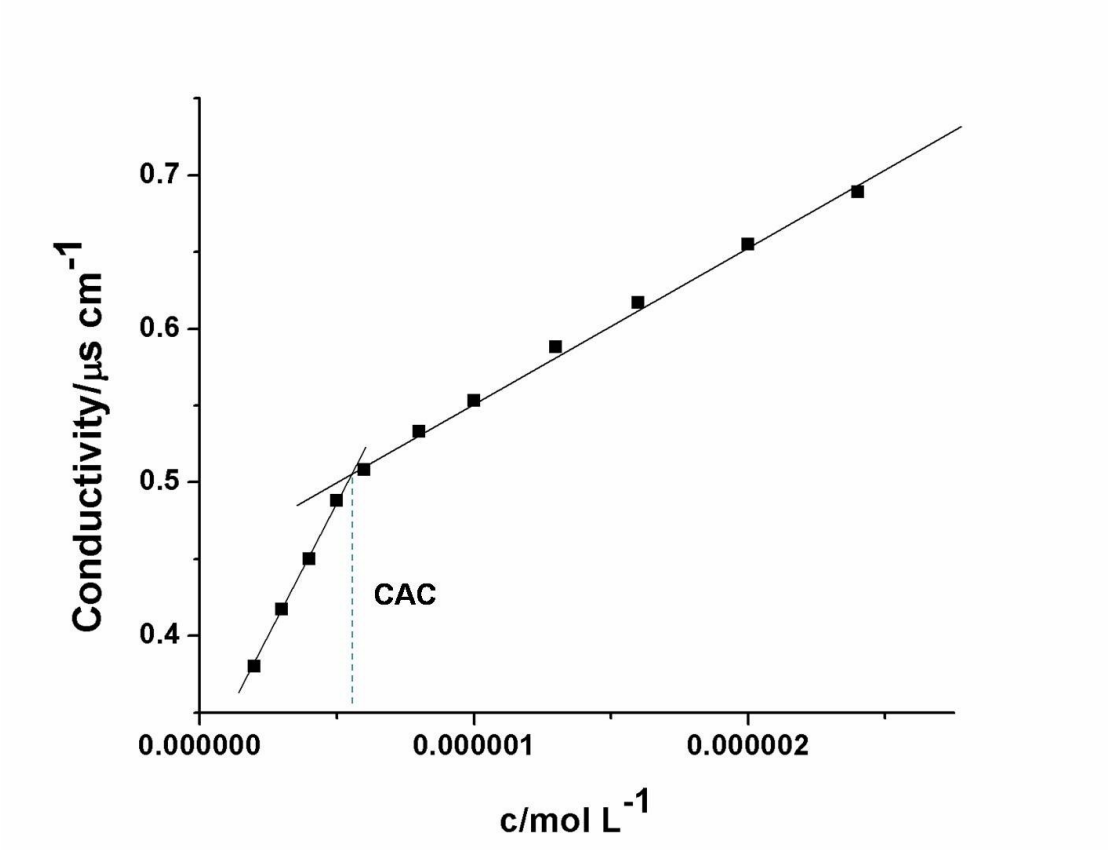

Fig. S7. The concentration-dependent conductivity of **A** in aqueous solutions. The critical aggregation concentration (CAC) was determined to be 5.49×10^{-7} M.

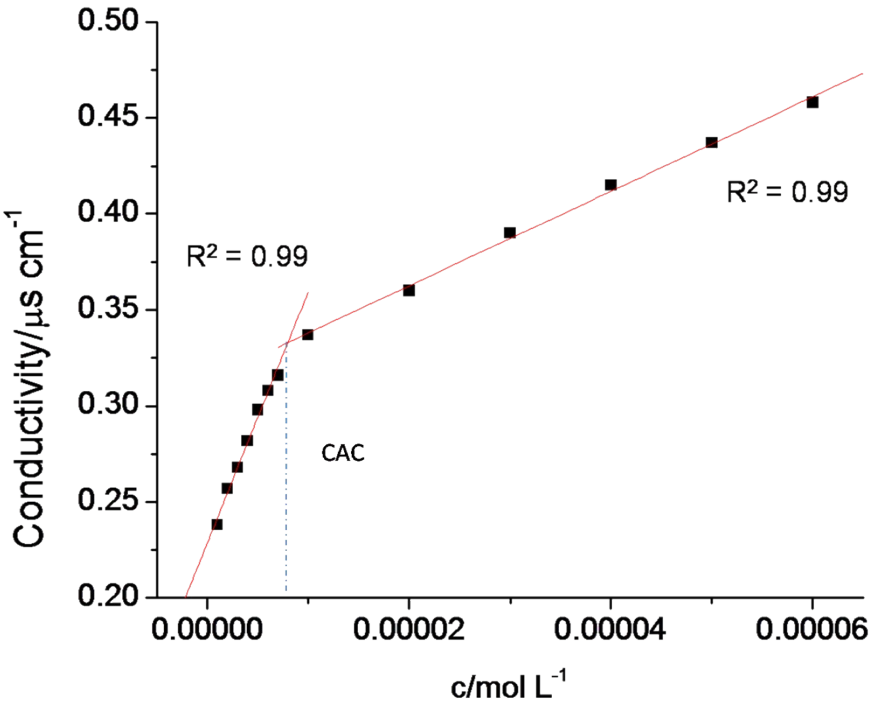

Fig. S8. The concentration-dependent conductivity of **G1@A** in aqueous solutions. The critical aggregation concentration value was determined to be 7.95×10^{-6} M.

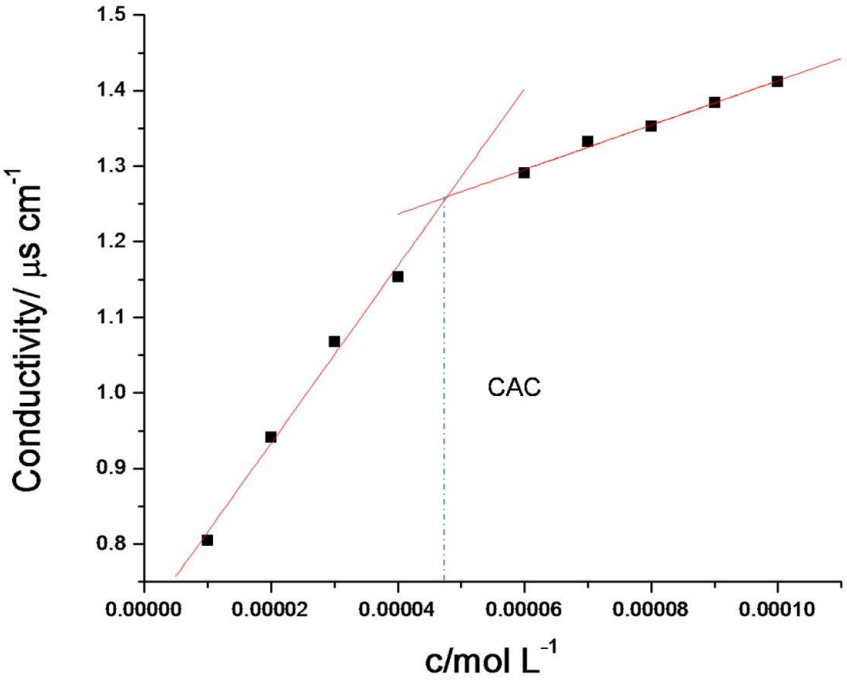

Fig. S9. The concentration-dependent conductivity of **WSP5⊃G1@A** in aqueous solutions. The critical aggregation concentration value was determined to be 4.74×10^{-5} M.

*5 Dynamic light scattering (DLS) result of **WSP5⊃G1@A***

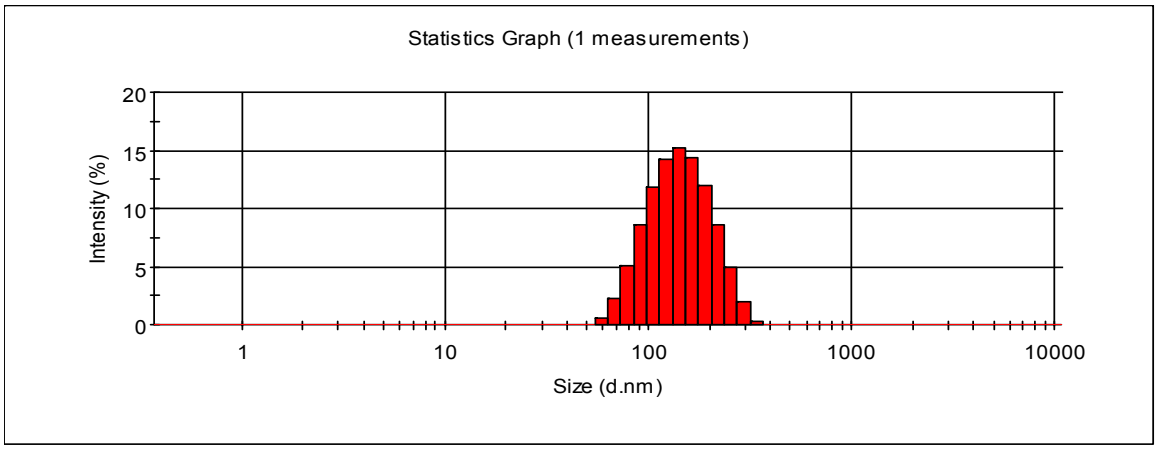

Fig. S10. DLS result of **WSP5⊃G1@A** with an aqueous solution of 1.00×10^{-4} M **WSP5** and 1.00×10^{-4} M **G1@A**.

*6 Fluorscence spectra of a solution of **WSP5⊃G1@A** upon the titration with different diols in aqueous solution*

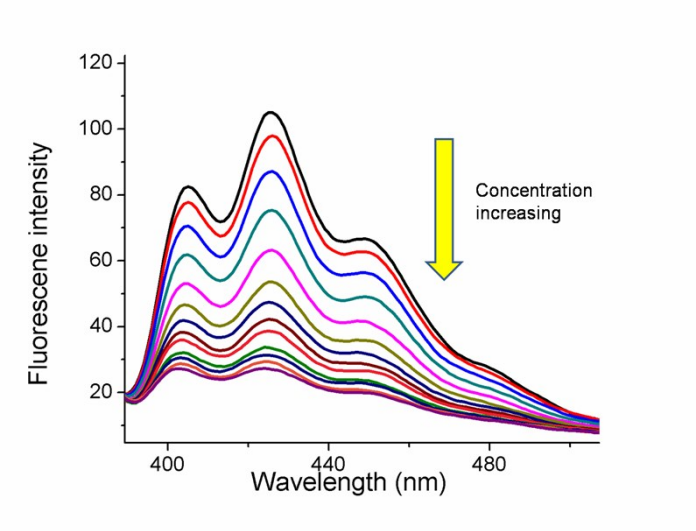

Fig. S11. The changes in fluorescence intensity of **WSP5⊃G1@A** (1.00×10^{-4} M) upon the titration of triethanolamine (0.00, 0.10, 0.30, 0.60, 1.00, 1.50, 2.00, 2.50, 3.00, 4.00, 5.00, 6.00, 7.00 equiv.) in aqueous solution (λ_{ex} = 370 nm).

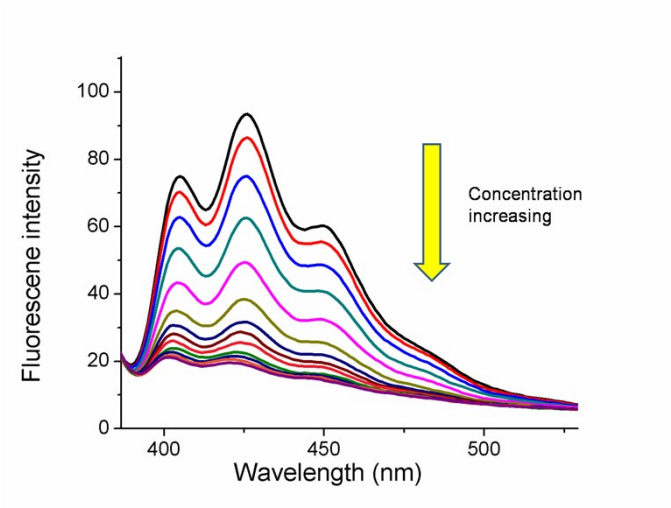

Fig. S12. The changes in fluorescence intensity of **WSP5⊃G1@A** (1.00×10^{-4} M) upon the titration of diethanolamine (0.00, 0.10, 0.30, 0.60, 1.00, 1.50, 2.00, 2.50, 3.00, 4.00, 5.00, 6.00, 7.00 equiv.) in aqueous solution (λ_{ex} = 370 nm).

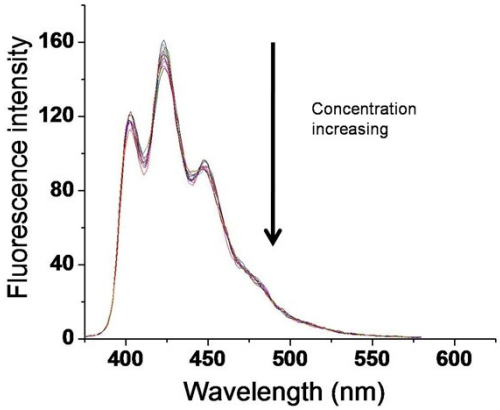

Fig. S13. The changes in fluorescence intensity of **WSP5⊃G1@A** (1.00×10^{-4} M) upon the titration of ethylene glycol (0.00, 0.10, 0.30, 0.60, 1.00, 1.50, 2.00, 2.50, 3.00, 4.00, 5.00, 6.00, 7.00 equiv.) in aqueous solution (λ_{ex} = 370 nm).

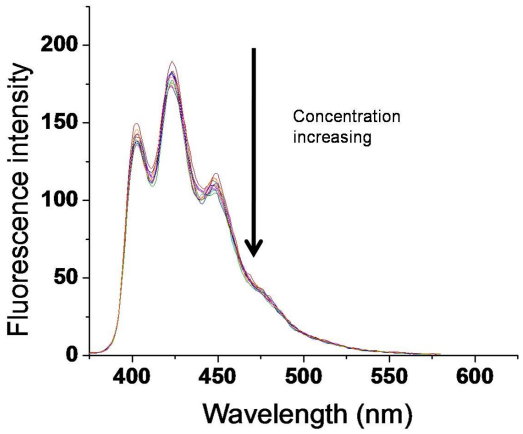

Fig. S14. The changes in fluorescence intensity of **WSP5⊃G1@A** (1.00×10^{-4} M) upon the titration of 2,2-dimethypropylene glycol (0.00, 0.10, 0.30, 0.60, 1.00, 1.50, 2.00, 2.50, 3.00, 4.00, 5.00, 6.00, 7.00 equiv.) in aqueous solution (λ_{ex} = 370 nm).

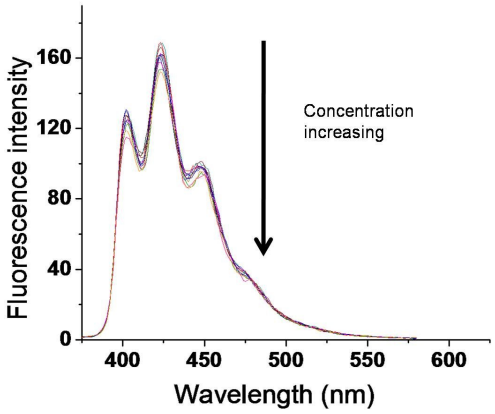

Fig. S15. The changes in fluorescence intensity of **WSP5⊃G1@A** (1.00×10^{-4} M) upon the titration of propylene glycol (0.00, 0.10, 0.30, 0.60, 1.00, 1.50, 2.00, 2.50, 3.00, 4.00, 5.00, 6.00, 7.00 equiv.) in aqueous solution (λ_{ex} = 370 nm).

*7. The morphology changes of **G1@A** upon gradual addition of **WSP5***

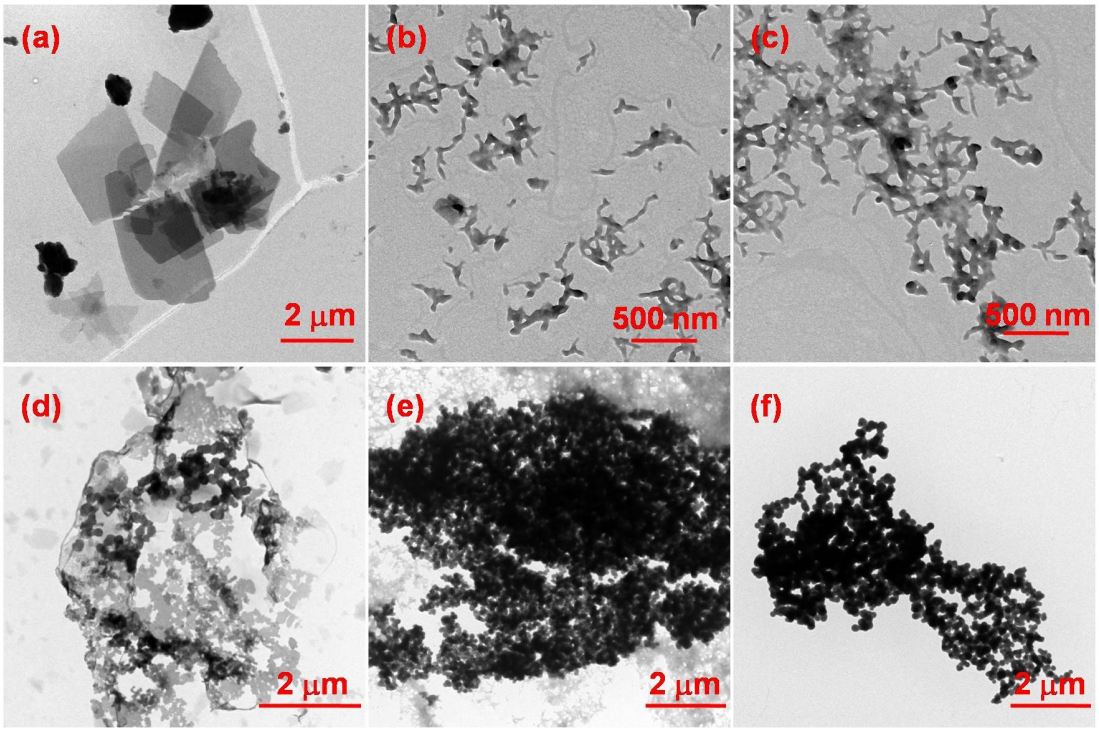

Fig. S16. The morphology changes of 1.00×10^{-4} M **G1@A** upon gradual addition of 1 equiv. of **WSP5**. Accompanied with gradual addtion of **WSP5**, the nanosheets of **G1@A** first

transformed into an intermediate state nanoribbon structures and finally turned into nanoparticles.

*8. The aggregate morphology changes of **WSP5⊃G1@A** upon gradual addition of diols **A1***

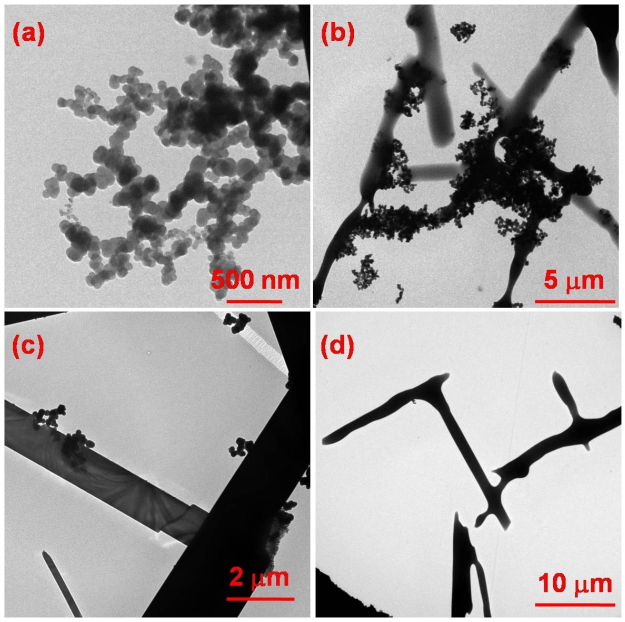

Fig. S17. The self-assembly morphology of (a) 1.00 × 10^{-4} M **WSP5⊃G1@A**; (b) 1.00 × 10^{-4} M **WSP5⊃G1@A** with 1.0 equiv. of **A1**; (c) 1.00 × 10^{-4} M **WSP5⊃G1@A** with 2.0 equiv. of **A1**; (d) 1.00 × 10^{-4} M **WSP5⊃G1@A** with 3.0 equiv. of **A1**.

*9. Scanning electron microscope (SEM) image of **A***

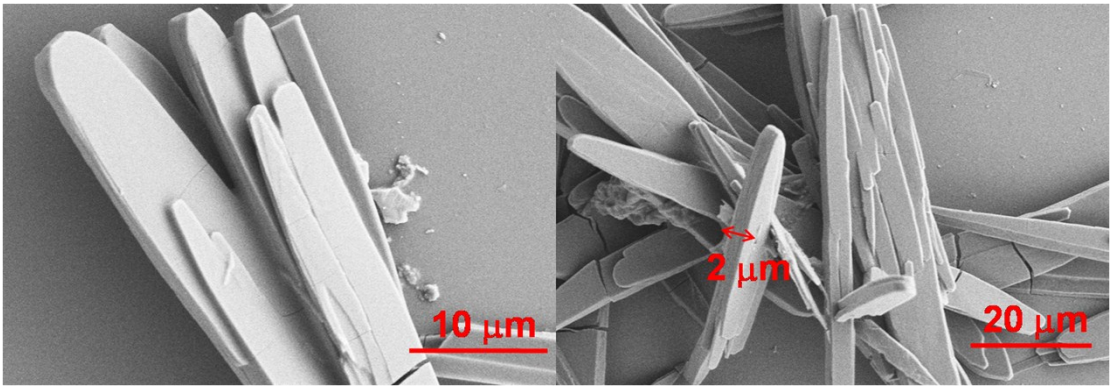

Fig. S18. SEM images of **A** aggregates.

*10. Atomic force microscope (AFM) image of **G1@A***

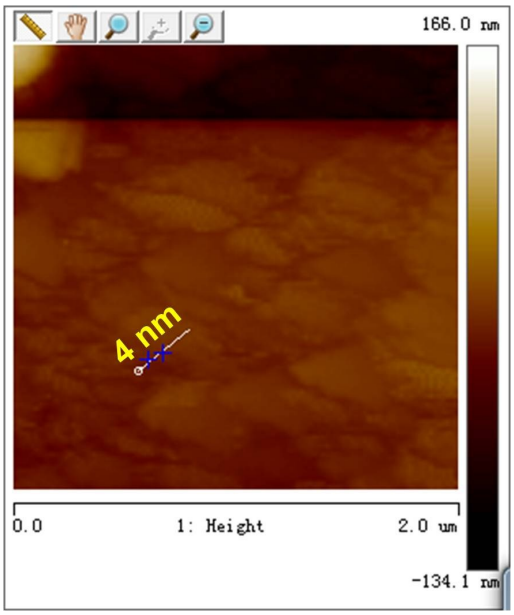

Fig. S19. AFM image of **G1@A** aggregates.

*10 Cartoon representation of the formation of the self-assembly structure from **G1@A** and **WSP5***

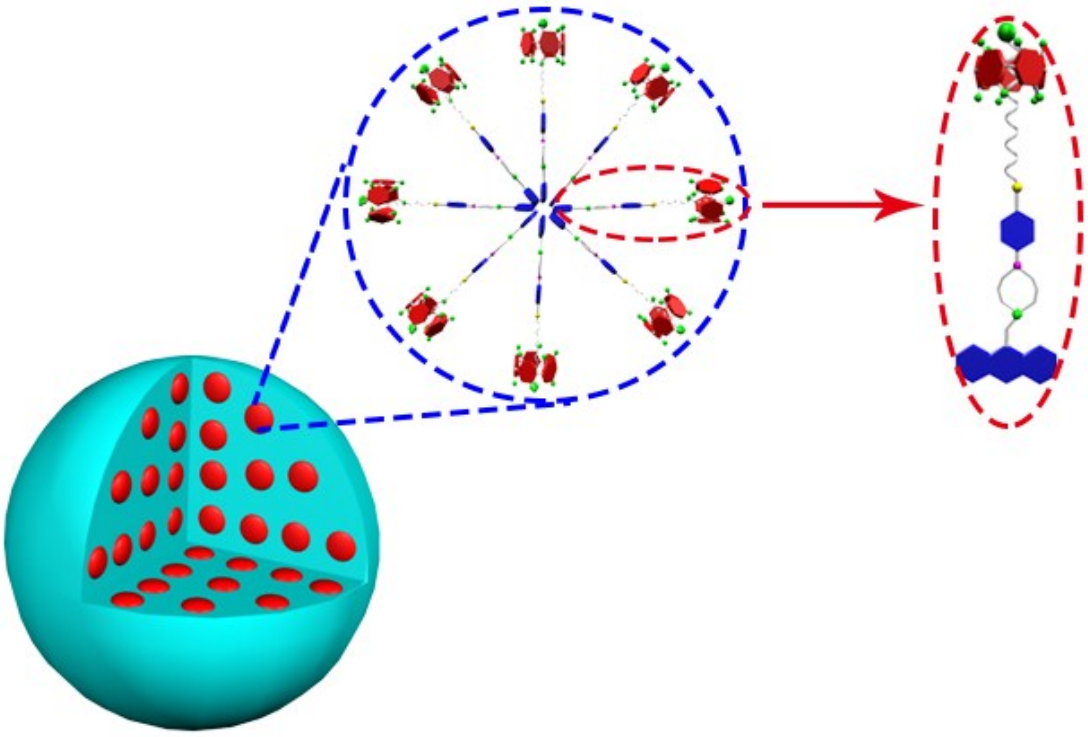

.

Fig. S20. Cartoon representation of the formation of the self-assembly structure from **G1@A** and **WSP5**.

11. *References*:

S1. M. Kozaki, Y. Ninomiya, S. Suzuki and K. Okada, *Tetrahedron Lett.,* 2013, **54**, 3658–3661.

S2. T. Ogoshi, M. Hashizume, T. Yamagishi and Y. Nakamoto, *Chem. Commun.*, 2010, **46**, 3708–3710.